

Article

Projected Water Scarcity and Hydrological Extremes in the Yellow River Basin in the 21st Century under SSP-RCP Scenarios

Lyuliu Liu ^{1,*} , Chan Xiao ¹ and Yihua Liu ²¹ National Climate Center, China Meteorological Administration, Beijing 100081, China² Climate Center of Qinghai, Xining 810001, China

* Correspondence: liull@cma.gov.cn; Tel.: +86-10-58995906

Abstract: This study investigated the potential impacts of climate change on water scarcity and hydrological extremes in the Yellow River Basin in the near-term (2026–2050), mid-term (2051–2075), and long-term (2076–2100) periods under three combined pathways of Shared Socioeconomic Pathways (SSPs) and Representative Concentration Pathways (RCPs) SSP1–2.6, SSP2–4.5, and SSP5–8.5 relative to the reference period (1986–2010), based on the runoff simulation through the Huayuankou hydrological station using the HBV-D hydrological model, which was forced by a statistically down-scaling dataset. The results indicate that water shortage would still threaten the Yellow River because annual runoff will remain below 1000 m³/year, although water scarcity would be alleviated to some degree. More and larger floods will happen in summer in the 21st century, especially in the long-term period under the SSP5–8.5 scenario. More Hydrological droughts will occur during July–October, and some extreme droughts would likely exceed the historical largest magnitudes in July and August in the long term under the SSP5–8.5 scenario.

Keywords: climate change impacts; water scarcity; hydrological drought; flood; Yellow River



Citation: Liu, L.; Xiao, C.; Liu, Y. Projected Water Scarcity and Hydrological Extremes in the Yellow River Basin in the 21st Century under SSP-RCP Scenarios. *Water* **2023**, *15*, 446. <https://doi.org/10.3390/w15030446>

Academic Editors: João Filipe Santos and Yaning Chen

Received: 15 December 2022

Revised: 13 January 2023

Accepted: 18 January 2023

Published: 22 January 2023



Copyright: © 2023 by the authors. Licensee MDPI, Basel, Switzerland. This article is an open access article distributed under the terms and conditions of the Creative Commons Attribution (CC BY) license (<https://creativecommons.org/licenses/by/4.0/>).

1. Introduction

The Yellow River is China's second-largest river in terms of length and watershed area. It supports 30.3% of the national population and represents 2.6% of the national total water resources [1]. The river is scarce in water resources, with a per capita water resource of approximately 579 m³ that includes 485 m³ of surface water resources and was projected to be at risk of water scarcity in 2021–2050 [2,3]. The Yellow River Basin experiences severe droughts and frequent floods. In past decades, most of the basin is considered to have a progressively drier transition based on the standardized precipitation evapotranspiration index and the Palmer drought index [4–6]; however, a contrary change has been identified in western parts of the Yellow River [7,8]. In much of the basin, the area and intensity of meteorological droughts would increase between 2040 and 2060 [9], but the duration and intensity of such events are expected to decrease in the source area [10]. The river is also known for its devastating floods and extremely high sediment load [11], and the occurrence of especially large floods and heavy sediment loads are concentrated in July and August [12]. In comparison with the historical period, the river is expected to have a higher risk of floods in the future [13]. Therefore, a major task for hydrological designers and planners is to investigate potential future changes in runoff, especially in terms of hydrological extremes such as droughts and floods. The most common method to explore the potential changes in hydrological variables, such as runoff at various temporal scales, hydrological drought, and flood, is based on the runoff simulations by the hydrological model forced by GCMs.

Hydrological drought has negative impacts on the quantity and quality of water [14]. It is an extreme condition reflecting the extension and development of meteorological

drought and agricultural drought [15]. One of the most well-known hydrological drought indexes is the standardized runoff/streamflow index [16–19]. Its calculation and explanation are similar to those of the standardized meteorological drought index used operationally by the World Meteorological Organization. Previous studies of the Yellow River Basin have investigated meteorological or agricultural droughts [4–6,20] or multivariate droughts [21,22]. Few studies explored the potential for future hydrological drought, although some studies analyzed hydrological drought in the Yellow River Basin based on streamflow records [21,23,24].

For floods, their changes in frequency and magnitude are of wide concern in the field of research on future disaster risk reduction and are often assessed using indexes such as the annual maximum runoff for 1, 3, 5, 7, or more days, e.g., [25,26], or the peak-over-threshold floods for an average rate of a specified number of times per year, e.g., [2,27]) at various return periods such as 100, 50, 30, or 20 years [28–30] relative to the reference period. For the Yellow River Basin, most previous studies analyzed the characteristics of extreme floods [31–33], explored the changes in magnitude and/or frequency of historical floods [31,34,35], or projected the potential flood risk [2,36] under Representative Concentration Pathways (RCPs).

GCM is the most popular tool to project future climate and to conjunct the downscaling techniques to the projection of hydrological variables. However, it is generally believed that different GCMs have their specific accuracy and reliability and that ensemble mean coupling with different GCMs provides more accurate climate change information [37,38]. The study aimed to explore the potential hydrological risk with indexes of water scarcity, hydrological drought, and floods in the Yellow River Basin during the 21st century under combined pathways of Shared Socioeconomic Pathways (SSPs) and RCPs, based on the hydrological simulation forced by global climate models (GCMs) in the Coupled Model Intercomparison Project phase 6 (CMIP6) (<https://esgf-node.llnl.gov/search/cmip6/>).

This study applied more indexes, longer time scales, and a greater number of GCMs than any previously singly related study. Moreover, the applied atmospheric forcing is the latest information that is from CMIP6 GCMs, which outperforms CMIP5 [39]. Moreover, the simulations of CMIP6 GCM were bias-corrected and spatial disaggregating in China. This processing improves the climate simulation by CMIP6 GCMs in the Yellow River Basin and China [40,41]. Moreover, SSP-RCP scenarios rather than RCP scenarios were applied, and the period of projection was extended to 2100 rather than to 2050 [2,36]. These are the innovation of this study.

2. Materials and Methods

2.1. Study Region

The Yellow River Basin (32°10′–41°50′ N, 90°53′–119°05′ E) covers an area of approximately 79.5×10^4 km², which includes an arid climate region in the northwest, a semiarid region in the central area, and a humid region in the southeast. Annual mean temperature varies from −3.4 to 15.0 °C, and the areal mean value is 8.1–10.5 °C. Annual mean precipitation varies from 144.5 mm in the arid region to 1066.4 mm in the humid region, and the areal mean value is 341–703 mm. Floods occur mainly during July–October, affected by seasonal precipitation patterns. This study focused on the upper watershed of the Huayuankou hydrological station (Figure 1a), which marks the division between the middle and lower reaches of the Yellow River and accounts for 91.8% of the entire area of the Yellow River Basin. More than 170 medium or large reservoirs have been constructed and operated. The streamflow through Huayuankou Station can be reduced from 42,300 to 22,600 m³/s for a 1-in-1000-year flood and from 29,200 m³/s to 15,700 m³/s for a 1-in-100-year flood by the joint operation of upstream reservoirs [39].

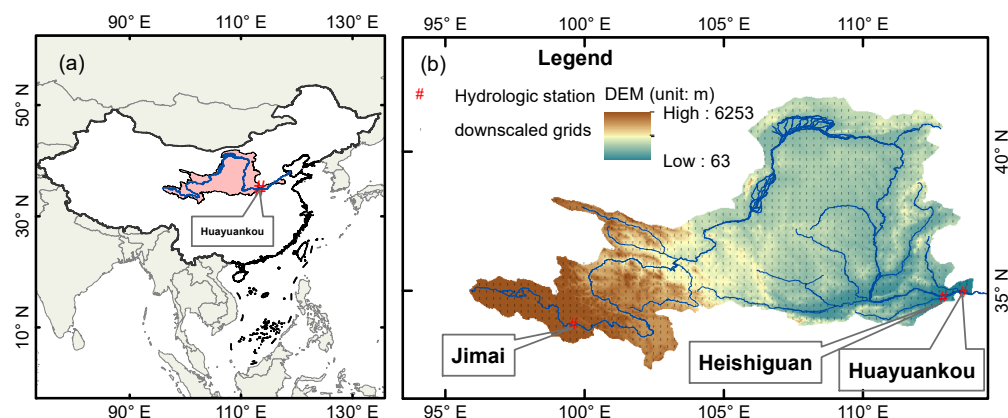


Figure 1. Location of (a) the Yellow River Basin and (b) three hydrological stations, together with basin topography and the grid of the downscaled climate dataset used in this study.

2.2. Datasets

The statistical downscaled datasets with $0.25^\circ \times 0.25^\circ$ resolution (Figure 1b) were developed by the National Climate Center of the China Meteorological Administration. The datasets comprise daily precipitation, daily mean, maximum and minimum temperature from 1986 to 2014, and projection from 2015 to 2100 under SSP1–2.6, SSP2–4.5, and SSP5–8.5 scenarios [41]. The datasets were set up by spatial disaggregating and bias-correcting with equal distance cumulative distribution function based on 13 CMIP6 GCMs (Table 1). The reproducibility of the spatial pattern of the downscaled datasets and raw simulations of CMIP6 GCMs has ever assessed over China [41] and the Yellow River Basin [40]. The assessments reveal that downscaling improved the spatial distributions of annual precipitation and extreme climate events and that it possessed higher spatial pattern correlations and greater Taylor Skill scores no matter single model or multi-model ensemble compared with the raw simulations of GCMs. In the study, the series of daily precipitation and daily mean temperature was used to force the HBV-D hydrological model.

The population data were obtained from the Science Data Bank (<https://cstr.cn/31253.11.sciencedb.01683>) [42]. They are the latest population information in China for 2010–2100 under the SSP1, SSP2, and SSP5 scenarios and have a resolution of $0.5^\circ \times 0.5^\circ$. They were developed using the multidimensional population–development–environment (PDE) model [43] with improved localized parameters [44]. The steps to project population with PDE refer to [2]. The PDE, with gradually improved parameters in China, even supported various research on the impacts, risks, and adaptation of climate change [2,45–48]. The population data applied here were the mean by aggregating the values of each grid in the study area. They were used to calculate the water scarcity indicator.

The data of monthly observed runoff for 1957–1997 through Jimai station, for 1970–2000 through Heishiguan, and monthly naturalized runoff for 1952–1998 through Huayuankou were from the Yellow River Resources Bureau. They are used to calibrate and validate the hydrological model.

2.3. Hydrological Model

In this study, the hydrological model HBV-D was used to simulate runoff. Its prototype is a lumped hydrological model developed by Swedish Meteorological and Hydrological Institute in the 1970s. Various versions of the HBV model have been developed and used worldwide since then [49]. HBV-D is a semi-distributed hydrological model, which is one of the derivations of the original HBV model. It has physically sound evapotranspiration schemes and descriptions of land cover characteristics. It is appropriate for the investigation of the hydrological impacts of climate change on large river basins [50]. The HBV-D model has been applied to estimate the precipitation threshold of flood disasters [51,52] and to predict/project runoff for tributaries [2,53–55] in the upper and middle reaches of the Yellow River.

Table 1. Details of the CMIP6 models used in this study.

ID	Model Name	Affiliated Country and Research Unit	Atmos. Lat/Lon Grid (°)
1	ACCESS-CM2	Commonwealth Scientific and Industrial Research Organisation, and Australian Research Council of Excellence for Climate System Science (Australia)	1.2° × 1.8°
2	ACCESS-ESM1-5	Commonwealth Scientific and Industrial Research Organisation(Australia)	1.2° × 1.8°
3	BCC-CSM2-MR	Beijing Climate Center, China Meteorological Administration (China)	1.1° × 1.1°
4	CanESM5	Canadian Centre for Climate Modelling and Analysis (Canada)	2.8 × 2.8
5	CNRM-CM6-1	Centre National de Recherches Météorologiques, Centre Européen de Recherche et de Formation Avancée en Calcul Scientifique (France)	1.4 × 1.4
6	CNRM-ESM2-1	Centre National de Recherches Météorologiques, Centre Européen de Recherche et de Formation Avancée en Calcul Scientifique (France)	1.4 × 1.4
7	HadGEM3-GC31-LL	Met Office Hadley Centre (United Kingdom)	1.3 × 1.9
8	INM-CM4-8	Institute for Numerical Mathematics, Russian Academy of Science (Russia)	1.5 × 2.0
9	INM-CM5-0	Institute for Numerical Mathematics, Russian Academy of Science (Russia)	1.5 × 1.5
10	IPSL-CM6A-LR	Institut Pierre Simon Laplace (France)	1.3 × 2.5
11	MIROC6	Japan Agency for Marine–Earth Science and Technology, Atmosphere and Ocean Research Institute (The University of Tokyo), National Institute for Environmental Studies, and RIKEN Center for Computational Science (Japan)	1.4 × 1.4
12	MPI-ESM1-2-HR	Max Planck Institute for Meteorology (Germany)	0.9 × 0.9
13	MRI-ESM2-0	Meteorological Research Institute (Japan)	1.1 × 1.1

The nonlinear parameter estimation and optimization package PEST was used to calibrate the HBV-D model using monthly runoff through the Huayuankou Station during 1952–1990 and to reference the parameters calibrated for some tributaries in previous research [2,40,51,52,54,55]. PEST applies a robust Gauss–Marquardt–Levenberg algorithm and combines the advantages of the inverse Hessian Method and the steep decent method [56,57]. The calibrated HBV-D was further validated using monthly runoff through Huayuankou Station, Jimai Station, and Heishiguan Station. The Jimai Station and the Heishiguan are on the mainstream in the source area and on a tributary of the middle Yellow River (Figure 1b), respectively. Selecting the two stations is to evaluate the accuracy of spatial pattern simulation for runoff of the HBV model.

2.4. Projection of Hydrological Variables

Water scarcity, hydrological droughts, and floods were projected with indices using the series of natural runoff simulated by calibrated HBV-D. The water scarcity on the annual scale was assessed with the water scarcity indicator (WSI), which is the per capita availability of renewable freshwater resources [58]. It is suitable for assessing the impact of climate change on physical water scarcity [59]. Water scarcity is considered to occur when the indicator falls below 1000 m³/year. A state of absolute scarcity is considered to occur when the indicator is below 500 m³/year [60]. To correct the bias in the projected annual water stress, the projected anomaly was added to the observed per capita surface water resources in 2010 with the same approach as in [2]. At the monthly scale, relative water scarcity will occur if the monthly runoff reduces by more than 20% of the reference.

Hydrological droughts were assessed with a standardized runoff index (SRI), which has been used previously [61–63]. In this study, SRI was computed following the procedure to calculate the standardized precipitation index [64] by replacing precipitation records with runoff records. Therefore, the classes or states used to describe hydrological drought were

identical to those adopted in the standardized precipitation index, as listed in Table 2. This classification allows comparison with other SRI values temporally and spatially. This study projected hydrological droughts on the 12-month time scale (SRI-12), as recommended by Mercado et al. [65].

Table 2. Classification of drought conditions according to the SRI.

SRI Values	Classifications
$SRI \geq 2.0$	Extremely wet
$1.5 \leq SRI < 2.0$	Very wet
$1.0 \leq SRI < 1.5$	Moderately wet
$-1.0 \leq SRI < 1.0$	Near normal
$-1.5 \leq SRI < -1.0$	Moderately dry
$-2.0 \leq SRI < -1.5$	Severely dry
$SRI < -2.0$	Extreme dry

Floods were resampled using the peak-over-threshold (POT) method for an average rate of three times per year. Projected floods were assessed using the return period and magnitude in the near-term (2026–2050), mid-term (2051–2075), and long-term (2076–2100) periods under the SSP1–2.6, SSP2–4.5, and SSP5–8.5 scenarios for 1-in-30-year events. The return period and magnitude were estimated using Generalized Pareto Distribution (GPD), which can be successfully fitted to the magnitudes and return periods of the POT floods [66,67]. The projected changes in flood magnitude were estimated based on the anomaly percentage relative to a reference period (1986–2010).

3. Results

3.1. Performance Assessment of HBV-D

As listed in Table 3, the Nash–Sutcliffe efficiency (E_{ns}) was greater than 0.50, the coefficient of determination (R^2) greater than 0.6, and the volume bias ($PBIAS$) within the range of -25% to 25% for the three stations. It was judged that the HBV-D model is satisfactory in simulating natural runoff through the Huayuankou hydrological station according to the evaluation criteria [68]. Thus it was used in this study to simulate natural runoff through the Huayuankou Station without considering human activities such as reservoir regulation and water extraction from the Yellow River. However, there is a pit for assessing the impacts of climate change on the spatial patterns of runoff in such a large basin. This leads to this study's focus on the changes in the runoff for the basin but not the changes in the spatial pattern of runoff.

Table 3. Evaluation of HBV-D performance for monthly simulation through three hydrological stations in the Yellow River Basin.

Station	Period	E_{ns}	R^2	$PBIAS(\%)$
Huayuankou	Calibration (1952–1990)	0.74	0.86	3.9
	Verification (1991–2012)	0.71	0.86	5.3
Jimai	Verification (1959–1997)	0.55	0.78	22
Heishiguan	Verification (1970–2000)	0.72	0.88	18

3.2. Changes in Water Scarcity

Annual water scarcity per capita in terms of the ensemble median will vary within the range of $511\text{--}828\text{ m}^3$ for the near-, mid-, and long-term periods under the SSP1–2.6, SSP2–4.5, and SSP5–8.5 scenarios (Table 4). The rate of change will be fastest under the SSP5–8.5 scenario and slowest under the SSP2–4.5 scenario and will increase more rapidly over time. From the value of 485 m^3 in the reference period, the median value will increase to 541 m^3 for the near-term period under the SSP1–2.6 scenario and increase to 828 m^3 for the long-term period under the SSP5–8.5 scenario. Some projections suggest that the value will even exceed 1000 m^3 , while other projections indicate that the value will be below

500 m³. It suggests that water scarcity could be alleviated to some degree, but the risk of absolute scarcity will be extremely high, and the state of water scarcity will continue over the coming decades in the 21st century.

Table 4. Projected annual runoff per capita for the near-, mid-, and long-term periods under the SSP1–2.6, SSP2–4.5, and SSP5–8.5 scenarios.

Period	Per Capita Annual Runoff: Median [min, max] (m ³)		
	SSP1–2.6	SSP2–4.5	SSP5–8.5
2026–2050	541 [373, 746]	511 [345, 826]	524 [399, 861]
2051–2075	607 [450, 1098]	528 [359, 1102]	641 [394, 1028]
2076–2100	788 [478, 1318]	583 [428, 1112]	828 [552, 1999]

Under most projections, runoff in most months for the near-term period will be within the range of –20% to 20% relative to the value of the reference period (Figure 2), but the number and the magnitude of the monthly increase will be greater than the decrease. Moreover, the increase will become faster over time and faster under the higher scenario than the lower scenario. For the mid-term and long-term periods, approximately half of the projections indicate an increase in monthly runoff by more than 20% in December, January, and September under the SSP5–8.5 and SSP2–4.5 scenarios. However, approximately half of the projections indicate that runoff will be within normal conditions in the transition season from winter to spring (February and March), summer (June–August), and mid-late autumn (October and November) in the future three periods under the SSP2–4.5 and SSP5–8.5 scenarios. These projections suggest a higher probability of water scarcity alleviation than worsening for mid-late winter and early autumn in the 21st century.

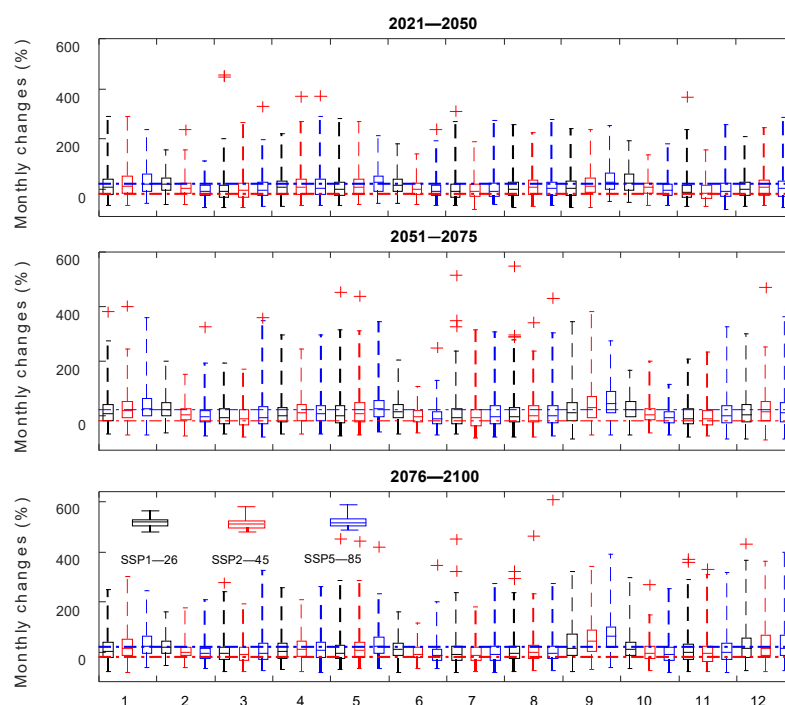


Figure 2. Projected change in monthly runoff (%) relative to the reference period for the near-, mid-, and long-term periods under the SSP1–2.6, SSP2–4.5, and SSP5–8.5 scenarios (red and blue lines represent –20% and 20% of the reference value, respectively. The outliers are marked with red +).

3.3. Changes in Hydrological Droughts

As shown in Figure 3, the median of monthly SRI-12 will increase by 7% at least, even by more than 2-fold of the reference for all months in the near-, mid-, and long-term under the SSP1–2.6, SSP2–4.5, and SSP5–8.5 scenarios except for August for mid-term under

SSP1–2.6 and long-term under SSP5–8.5, but at least 50% projections still within the near normal condition.

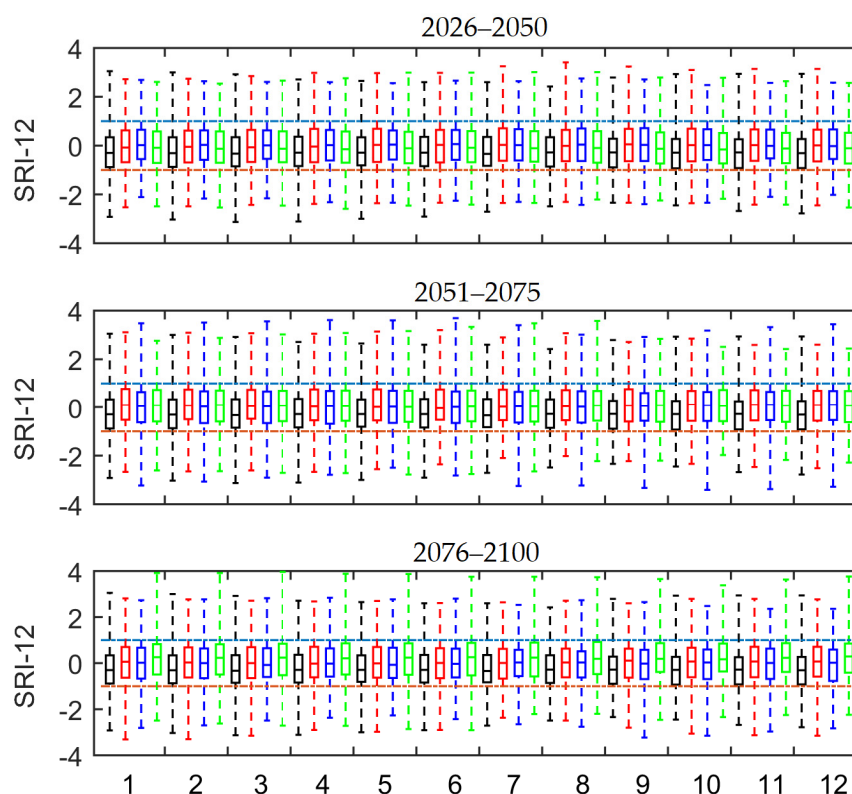


Figure 3. Projected SRI-12 for the near-, mid-, and long-term periods under the SSP1–2.6, SSP2–4.5, and SSP5–8.5 scenarios (black, red, blue, and green boxes represent the reference period, SSP1–2.6, SSP2–4.5, and SSP5–8.5 scenarios, respectively).

Fewer hydrological droughts will occur in November–June, while more will occur during July–October. Specifically, more droughts will occur in July–September under the SSP2–4.5 scenario, in July and August under the SSP1–2.6 scenario for the near-, mid-, and long-term periods, in August and September under the SSP5–8.5 scenario for the near- and mid-term periods, and in October under the SSP1–2.6 and SSP2–4.5 scenarios for the mid-term period (Table 5).

Table 5 further shows that moderate droughts will occur more frequently in July for the near- and mid-term periods under the SSP1–2.6 scenario and for the long-term under the other two scenarios, in August for the mid-term and long-term under the SSP1–2.6 scenario, and for the future three periods under the SSP2–4.5 scenario, and in August and September for the near- and mid-term periods under the SSP5–8.5 scenario. Severe droughts will occur more frequently in July for the long-term under the three scenarios, in August for the near-term and mid-term periods under the SSP5–8.5 scenario, in September for all three periods and three scenarios, and in August for the mid-term period under the SSP2–4.5 and SSP5–8.5 scenarios. Extreme droughts will occur more frequently in June for the long-term under the SSP2–4.5 and SSP5–8.5 scenarios, in July for almost all periods and scenarios except for the mid-term under SSP1–2.6 scenario, in September and October for the mid-term period under the SSP2–4.5 and long-term under the SSP2–4.5 and SSP5–8.5 scenarios, and in November for the mid-term and long-term periods under the SSP2–4.5 scenario.

Table 5. Changes in frequency (times) of SRI-12 relative to the reference period for the near-, mid-, and long-term periods under the SSP1–2.6, SSP2–4.5, and SSP5–8.5 scenarios.

Month	Scenario	Moderately Dry			Severely Dry			Extreme Dry		
		Near-Term	Mid-Term	Long-Term	Near-Term	Mid-Term	Long-Term	Near-Term	Mid-Term	Long-Term
6	ssp126	−14	−19	−17	−1	−8	−7	−4	−4	−28
	ssp245	−26	−21	−12	−8	−1	1	−6	0	−10
	ssp585	−14	−21	−5	−12	−3	−2	−4	−4	−5
7	ssp126	5	3	−8	0	−4	3	6	−1	−3
	ssp245	0	−1	13	1	−2	4	0	7	22
	ssp585	1	−5	5	−2	4	4	3	4	13
8	ssp126	−5	7	7	6	−1	−2	6	0	6
	ssp245	4	6	5	−3	7	−	1	3	17
	ssp585	10	7	−1	3	3	−2	4	3	0
9	ssp126	0	6	−8	7	8	2	−2	−2	−9
	ssp245	−2	−6	−4	6	7	10	−2	4	7
	ssp585	8	3	−8	10	10	4	0	−5	−2
10	ssp126	−6	−1	−9	2	3	−4	−2	−1	−17
	ssp245	−3	−5	−1	−7	3	−3	−3	−	−2
	ssp585	13	−1	−1	−4	−6	2	3	−4	6
11	ssp126	−2	−4	−4	0	−2	−10	−5	−4	−20
	ssp245	−4	−6	−7	−4	−1	−6	−8	2	−12
	ssp585	−8	−4	−11	4	−4	−7	−3	−7	−22

These suggest that fewer hydrological droughts will occur during November–June but more during July–October. Moreover, the probability of exceeding the historical maximum intensity will be higher in July and August than in other months.

The numbers of hydrological droughts exceeding the historical maximum intensity are shown in Figure 4. It is projected that extreme droughts with greater magnitude will occur in December–February and June–October during 2076–2100 under the SSP5–8.5 scenario, in July and August during 2026–2050 under the SSP5–8.5 scenario, and during 2056–2075 under the SSP2–4.5 scenario. The maximum probability would be approximately 1% in July under the SSP5–8.5 scenario and in August under the SSP1–2.6 and SSP5–8.5 scenarios for the long-term period. The probability will be lower in June–February and in April for certain periods under certain scenarios.

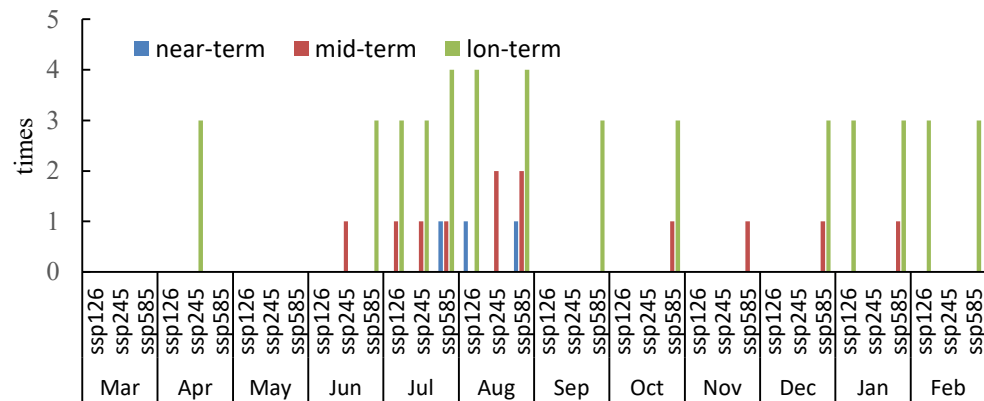


Figure 4. The number of hydrological droughts (SRI-12) exceeding the historical maximum intensity for the near-, mid-, and long-term periods under the SSP1–2.6, SSP2–4.5, and SSP5–8.5 scenarios.

3.4. Changes in Floods

Figure 5 shows that the magnitude of 1-in-30-year floods will increase, and the return period will decrease in the three future periods under the SSP1–2.6, SSP2–4.5, and SSP5–8.5 scenarios. The magnitude of floods will increase by 7.5%–11.8%, and the return period will decrease to 18.1–21.8 years in terms of the median for the near-term period under all three scenarios, but the magnitude will increase by 30.4% and the return period will decrease to 9.3 years in the long-term period under the SSP5–8.5 scenario (Table 6). It suggests that the Yellow River Basin will experience larger and more frequent floods in the future.

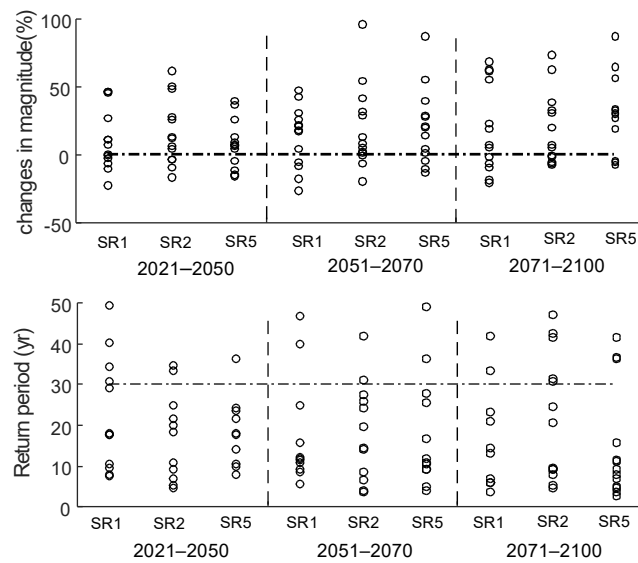


Figure 5. Projected magnitude and return period of 1-in-30-year floods for the near-, mid-, and long-term periods under the SSP1–2.6 (SR1), SSP2–4.5 (SR2), and SSP5–8.5 (SR3) scenarios.

Table 6. Magnitude and return period of 1-in-30-year floods for the near-, mid-, and long-term periods under the SSP1–2.6, SSP2–4.5, and SSP5–8.5 scenarios.

Period	Change in Magnitude of 1-in-30-Year Floods (%)			Return Period of 1-in-30-Year Floods		
	Median [min, max]			Median [min, max]		
	SSP1–2.6	SSP2–4.5	SSP5–8.5	SSP1–2.6	SSP2–4.5	SSP5–8.5
2026–2050	7.5 [−21.7, 46.8]	11.8 [−15.8, 61.5]	7.5 [−15.1, 40.1]	18.1 [7.5, 49.4]	20.0 [4.8, 87.0]	21.8 [8.2, 99.0]
2051–2075	16.8 [−25.6, 47.5]	8.5 [−19.1, 95.8]	19.6 [−13.3, 86.7]	12.1 [5.6, 213.7]	19.7 [3.7, 155.8]	12.0 [4.1, 75.7]
2076–2100	7.1 [−20.0, 68.4]	7.4 [−7.5, 73.1]	30.4 [−7.8, 107.3]	21.1 [3.7, 183.9]	20.9 [4.8, 47.2]	9.3 [2.8, 41.5]

4. Discussion

The findings of this study indicate that annual runoff per capita will likely increase in the 21st century, whereas it was ever projected to decrease [2,3] before 2050 under the RCP2.6, RCP4.5, and RCP8.5 scenarios. The contrasting conclusions could be attributed to the use of different reference periods and different projection periods. The reference period is 1976–2005 for reference [2] and 1961–1990 for reference [3]. However, all three studies confirm that water scarcity will be a major threat in the Yellow River Basin in the future.

The projected larger and more frequent floods are consistent with previous conclusions of a higher risk of floods [2,13] in the coming 30 years under the RCP2.6, RCP4.5, RCP6.0, and RCP8.5 scenarios. A higher risk of floods would present considerable socioeconomic challenges for the Yellow River Basin.

Water scarcity on annual and seasonal scales was explored in this study. However, it would be informative to develop another index to describe water scarcity because the annual runoff per capita is an index that considers only supply-side changes without consideration of social adaptability. Moreover, water scarcity on a monthly scale was assessed based on the changes in runoff relative to the reference period. It is an index of relative change and cannot reflect the condition of absolute water scarcity and social adaptability.

Uncertainty in the projected hydrological variables remains an ongoing issue. Generally, the structure, initial conditions, and parameters of the adopted climate model, hydrological model and population model, climate change scenarios, downscaling method, and climate variability represent the major potential sources of uncertainty. Many previous studies explored such uncertainties and reported that the importance of various sources of

uncertainty varies with region, projection period, and projected variables, but the uncertainties associated with climate models and greenhouse gas emission scenarios are usually dominant [69–74]. Here, the uncertainties associated with the GCM structure and climate scenarios were considered by using 13 GCMs of CMIP6 and 3 SSP-RCPs scenarios and population under three SSPs. The equilibrium climate sensitivity (ECS) of the 13 GCMs in the study ranges from 1.83 to 5.62 °C [75] and covers most of the ECS ranges of CMIP6 models [76], and can quantify the ranges and uncertainties contributed by GCMs. Moreover, most of the CMIP6 models have advantages over previous CMIP5 models in reproducing the interannual anomalous rainfall pattern over Eastern China [77]. Evaluation of the ability of 23 climate models from CMIP6 in simulating extreme climate events showed that the multi-model ensemble of CMIP6 can capture the spatial patterns of precipitation extremes pretty well over China [78].

Although Jimai station and Heishiguan Station were used to evaluate the accuracy of spatial pattern simulation for runoff of the HBV model, it is still a pit to validate the model in this large basin. The weakness of evaluation for the accuracy of spatial pattern simulation for runoff leads to this study's focus on the assessment of changes in the runoff for the basin and cannot further assess the changes in the spatial pattern of runoff. Moreover, the uncertainties associated with the hydrological model and the downscaling procedure were neglected because it is a too great challenge to attempt to examine all possible sources of uncertainty simultaneously. Ideally, additional hydrological models, downscaling methods, and GCMs should be incorporated into the projections to provide more convincing information. However, the downscaled climate forcing applied in this study is suitable for reproducing the climate of the Yellow River Basin [41], and the HBV-D model is capable of successfully simulating runoff through the Huayuankou Station. Therefore, the derived results can be considered to have important implications regarding water resources management in the context of climate change and population development.

5. Conclusions

This study projected that water scarcity in the Yellow River Basin will continue in the 21st century, although annual runoff per capita will increase to some degree in terms of the median and for most projections. For example, annual runoff per capita will increase to 828 m³/year in the long-term period under the SSP5–8.5 scenario from the value of 485 m³/year during the reference period.

The degree of water scarcity alleviation will vary with the season. Water scarcity will likely be alleviated for mid-late winter and early autumn in the 21st century. However, the runoff will be in normal condition for other months under most projections.

The Yellow River Basin will likely experience larger and more frequent floods in the 21st century. The risk will be highest in the long-term period under the SSP5–8.5 scenario, when the magnitude will increase by 30.4% and the return period will decrease to 9.3 years for 1-in-30-year floods.

Less hydrological droughts in terms of SRI-12 will occur in November–June, while more droughts will occur in July–October. Droughts exceeding the historical maximum intensity will likely occur in July and August in the long-term period.

In the future, in the context of slight water scarcity alleviation, hydrological extremes comprising severe floods and droughts will be encountered more frequently in the Yellow River Basin, with a greater risk of occurrence in summer. The projections of this study have implications for policymakers and water management planners regarding the mitigation of the negative impacts of climate change on the Yellow River Basin.

Author Contributions: Conceptualization, L.L.; Formal analysis, L.L.; Methodology, L.L.; Resources, C.X.; Supervision, C.X.; Writing—original draft, L.L. and Y.L.; Writing—review and editing, L.L. and Y.L. All authors have read and agreed to the published version of the manuscript.

Funding: This research was partially supported by the National Key Research and Development Program of China (No. 2016YFE010240004, 2018YFE019600004, and 2017YFA0605004), Special Funds

(Meteorology) for Scientific Research on Public Interest (No. GYH201406021), and Science and Technology Department Program of Qinghai (No. 2022-ZJ-767).

Institutional Review Board Statement: Not applicable.

Informed Consent Statement: Not applicable.

Data Availability Statement: All data generated or analyzed during this study are included in this published article.

Acknowledgments: The authors would like to thank the CMIP6 modeling groups for producing and making available their model output.

Conflicts of Interest: The authors declare no conflict of interest.

References

1. He, A.; Gong, K.; Zhang, Z.; Dong, W.; Feng, H.; Yu, Q.; He, J. What is the past, present, and future of scientific research on the Yellow River Basin? —A bibliometric analysis. *Agric. Water Manag.* **2022**, *262*, 107404. [[CrossRef](#)]
2. Liu, L.; Jiang, T.; Xu, H.; Wang, Y. Potential Threats from Variations of Hydrological Parameters to the Yellow River and Pearl River Basins in China over the Next 30 Years. *Water* **2018**, *10*, 883. [[CrossRef](#)]
3. Wang, G.; Qiao, C.; Liu, M.; Du, M.; Ye, T.; Wang, J. The future water resources regime of the Yellow River basin in the context of climate change. *Hydro-Sci. Eng.* **2020**, *2*, 1–8. (In Chinese)
4. Ma, M.; Ren, L.; Singh, V.; Yuan, F.; Chen, L.; Yang, X.; Liu, Y. Hydrologic model-based Palmer indices for drought characterization in the Yellow River basin, China. *Stoch. Environ. Res. Risk Assess.* **2016**, *30*, 1401–1420. [[CrossRef](#)]
5. Wang, Y.; Wang, S.; Zhao, W.; Liu, Y. The increasing contribution of potential evapotranspiration to severe droughts in the Yellow River basin. *J. Hydrol.* **2022**, *605*, 127310. [[CrossRef](#)]
6. Li, Y.; Jia, C.; Hu, Z.; Sun, J. Refined spatiotemporal analysis of drought characteristics under different characteristic variable matchings: A case study of the middle reaches of the Yellow River basin, China. *Environ. Sci. Pollut. Res.* **2022**, *29*, 60440–60458. [[CrossRef](#)]
7. Huang, T.; Lin, Q.; Wu, Z.; Wang, Y. Spatial and Temporal Characteristics of Drought in the Yellow River Basin and Their Correlation with ENSO. *Yellow River* **2021**, *43*, 52–58. (In Chinese)
8. Liu, Y.; Xue, W. Temporal and spatial evolution of agricultural drought and its natural recovery period in the Yellow River Basin. *Agric. Res. Arid. Areas* **2022**, *40*, 213–221. (In Chinese)
9. Ji, G. Geographical Calculation of Runoff Change and Drought and Flood Disasters Dynamics in the Yellow River Basin under Future Climate Change. Ph.D. Thesis, East China Normal University, Shanghai, China, 2020. (In Chinese)
10. Zhang, L.; Zheng, W.; Yang, X.; Wang, Y.; Zhang, M.; Yu, X. Temporal-spatial characteristics of drought in source region of Yellow River based on CMIP5 multi-mode ensemble and PDSI. *Water Resour. Prot.* **2019**, *35*, 95–99. (In Chinese)
11. Fan, X.; Shi, C.; Shao, W.; Zhou, Y. The suspended sediment dynamics in the Inner-Mongolia reaches of the upper Yellow River. *Catena* **2013**, *109*, 72–82. [[CrossRef](#)]
12. Ran, Q.; Zong, X.; Ye, S.; Gao, J.; Hong, Y. Dominant mechanism for annual maximum flood and sediment events generation in the Yellow River basin. *Catena* **2020**, *187*, 104376. [[CrossRef](#)]
13. Ding, Y.; Jiang, C.; Zhou, Z.; Gao, T.; Wang, S.; Zhang, X.; Cai, H.; Shi, H. Evaluation of precipitation and its time series components in CMIP6 over the Yellow River Basin. *Clim. Dyn.* **2022**. [[CrossRef](#)]
14. Ahmadi, B.; Ahmadalipour, A.; Moradkhani, H. Hydrological drought persistence and recovery over the CONUS: A multi-stage framework considering water quantity and quality. *Water Res.* **2019**, *150*, 97–110. [[CrossRef](#)] [[PubMed](#)]
15. He, Z.; Liang, H.; Yang, C.; Huang, F.; Zeng, X. Temporal-spatial evolution of the hydrologic drought characteristics of the karst drainage basins in South China. *Int. J. Appl. Earth Obs. Geoinf.* **2018**, *64*, 22–30. [[CrossRef](#)]
16. Shukla, S.; Wood, A. Use of a standardized runoff index for characterizing hydrologic drought. *Geophys. Res. Lett.* **2008**, *35*, L02405. [[CrossRef](#)]
17. Nalbantis, I. Evaluation of a Hydrological Drought Index. *Eur. Water* **2008**, *23*, 67–77.
18. Nalbantis, I.; Tsakiris, G. Assessment of hydrological drought revisited. *Water Resources. Manag.* **2009**, *23*, 881–897. [[CrossRef](#)]
19. Ahmadalipour, A.; Moradkhani, H.; Demirel, M. A comparative assessment of projected meteorological and hydrological droughts: Elucidating the role of temperature. *J. Hydrol.* **2017**, *553*, 785–797. [[CrossRef](#)]
20. Li, Y.; Chang, J.; Fan, J.; Yu, B. Agricultural drought evolution characteristics and driving mechanisms in the Yellow River Basin under climate and land use changes. *Trans. Chin. Soc. Agric. Eng.* **2021**, *37*, 84–93. (In Chinese)
21. Ren, L.; Shen, H.; Yuan, F.; Zhao, X.; Yang, X.; Zheng, P. Hydrological drought characteristics in the Weihe catchment in a changing environment. *Adv. Water Sci.* **2016**, *27*, 492–500. (In Chinese)
22. Wang, L.; Huang, S.; Huang, Q.; Fang, W.; Li, K.; Zhang, Y. Drought multivariable probability characteristics based on a multivariate standardized drought index in the Yellow River basin. *J. Nat. Disasters* **2019**, *28*, 70–80. (In Chinese) [[CrossRef](#)]
23. Ma, M.; Cheng, Y.; Cui, H.; Zang, H.; Wang, Z. Multivariate characteristics of streamflow drought at Tangnaihai station of the Yellow River. *J. North China Univ. Water Resour. Electr. Power (Nat. Sci. Ed.)* **2020**, *41*, 1–9. (In Chinese)

24. Yang, T.; Xi, Y.; Liu, W. Application of Drought Frequency Analysis Method Based on Copula in Tangnaihais Watershed. *Shanxi Water Resour.* **2020**, *6*, 15–18, 28. (In Chinese)
25. Villarini, G.; Smith, J.A.; Serinaldi, F.; Bales, J.; Bates, P.; Krajewski, W. Flood frequency analysis for nonstationary annual peak records in an urban drainage basin. *Adv. Water Resour.* **2009**, *32*, 1255–1266. [[CrossRef](#)]
26. Liu, L.; Jiang, T.; Xu, J.; Zhai, J.; Luo, Y. Responses of hydrological processes to climate change in the Zhujiang River Basin in the 21st century. *Adv. Clim. Chang. Res.* **2012**, *3*, 84–91. [[CrossRef](#)]
27. Eingrüber, N.; Korres, W. Climate change simulation and trend analysis of extreme precipitation and floods in the mesoscale Rur catchment in western Germany until 2099 using Statistical Downscaling Model (SDSM) and the Soil & Water Assessment Tool (SWAT model). *Sci. Total Environ.* **2022**, *838*, 155775. [[CrossRef](#)] [[PubMed](#)]
28. Hirabayashi, Y.; Mahendran, R.; Koirala, S.; Konoshima, L.; Yamazaki, D.; Watanabe, S.; Kim, H.; Kanae, S. Global flood risk under climate change. *Nat. Clim. Chang.* **2013**, *3*, 816–821. [[CrossRef](#)]
29. Dankers, R.; Arnell, N.W.; Clark, D.B.; Falloon, P.D.; Fekete, B.M.; Gosling, S.N.; Heinke, J.; Kim, H.; Masaki, Y.; Satoh, Y.; et al. First look at changes in flood hazard in the inter-sectoral impact model intercomparison project ensemble. *Prac. Natl. Acad. Sci. USA* **2014**, *111*, 3257–3261. [[CrossRef](#)] [[PubMed](#)]
30. Kundzewicz, Z.; Su, B.; Wang, Y.; Wang, G.; Wang, G.; Huang, J.; Jiang, T. Flood risk in a range of spatial perspectives –from global to local scales. *Nat. Hazards Earth Syst. Sci.* **2019**, *19*, 1319–1328. [[CrossRef](#)]
31. Peng, H.; Zheng, Y.; Shang, H. Analysis on Flood-variation Characteristics in Tangnaihe River and Its Upstream of the Yellow River. *J. North China Univ. Water Resour. Electr. Power (Nat. Sci. Ed.)* **2014**, *35*, 18–20. (In Chinese)
32. Zhang, J.; Liu, J.; Wang, Z.; Li, C. Analysis of Rainfall-Flood-Sediment Characteristics of the No.1 Flood in 2017 in the Yellow River. *Yellow River* **2017**, *39*, 14–17. (In Chinese)
33. Gao, X.; Li, J.; Sun, C. Flood Analysis of Ningxia Section of the Yellow River in 2018. *Ningxia J. Agric. For. Sci. Technol.* **2020**, *61*, 35–37. (In Chinese)
34. Bai, P.; Liu, X.; Liang, K.; Liu, C. Investigation of changes in the annual maximum flood in the Yellow River basin, China. *Quat. Int.* **2016**, *392*, 168–177. [[CrossRef](#)]
35. Zhao, Y.; Cao, W.; Hu, C.; Wang, Y.; Wang, Z.; Zhang, X.; Zhu, B.; Cheng, C.; Yin, X.; Liu, B.; et al. Analysis of changes in characteristics of flood and sediment yield in typical basins of the Yellow River under extreme rainfall events. *Catena* **2019**, *177*, 31–40. [[CrossRef](#)]
36. Wen, Y. Study on Future Extreme Climate Change in the Yellow River Basin and its Impact on Mid-Stream Flood Events. Master's Thesis, Zhengzhou University, Zhengzhou, China, 2020. (In Chinese)
37. Miao, C.; Duan, Q.; Sun, Q.; Huang, Y.; Kong, D.; Yang, T.; Ye, A.; Di, Z.; Gong, W. Assessment of CMIP5 climate models and projected temperature changes over Northern Eurasia. *Environ. Res. Lett.* **2014**, *9*, 055007. [[CrossRef](#)]
38. Zhang, Y.; Cheng Yang, T.; Jin, X.; Jia, Z.; Shen, J.; Wu, X. Assessment of climate change impacts on the hydro-wind-solar energy supply system. *Renew. Sustain. Energy Rev.* **2022**, *162*, 112480. [[CrossRef](#)]
39. Wei, X.; Cai, B.; Cao, B. Construction and achievements of flood control, drought relief and disaster systems in the Yellow River Basin. *China Flood Drought Manag.* **2019**, *29*, 43–53. (In Chinese)
40. Liu, L.; Wei, L.; Xu, Y.; Xin, X.; Xiao, C. Projection of climate change impacts on ecological flow in the Yellow River basin. *Adv. Water Sci.* **2021**, *32*, 824–833. (In Chinese)
41. Wei, L.; Liu, L.; Jing, C.; Wu, Y.; Xin, X.; Yang, B.; Tang, H.; Li, Y.; Wang, Y.; Zhang, T.; et al. Simulation and projection of climate extremes in China by a set of statistical downscaled data. *Int. J. Environ. Res. Public Health* **2022**, *19*, 6398. [[CrossRef](#)]
42. Jiang, T.; Su, B.; Wang, Y.; Wang, G.; Luo, Y.; Zhai, J.; Huang, J.; Jing, C.; Gao, M.; Lin, Q.; et al. Gridded datasets for population and economy under Shared Socioeconomic Pathways for 2020–2100. *Clim. Chang. Res.* **2022**, *18*, 381–383. (In Chinese)
43. Samir, K.; Lutz, W. The human core of the shared socioeconomic pathways: Population scenarios by age, sex and level of education for all countries to 2100. *Glob. Environ. Chang.* **2017**, *42*, 181–192.
44. Huang, J.; Qin, D.; Jiang, T.; Wang, Y.; Feng, Z.; Zhai, J.; Cao, L.; Chao, Q.; Xu, X.; Wang, G.; et al. Effect of fertility policy changes on the population structure and economy of China: From the perspective of the shared socioeconomic pathways. *Earth's Future* **2019**, *7*, 250–265. [[CrossRef](#)]
45. Jiang, T.; Zhao, J.; Jing, C.; Cao, L.; Wang, Y.; Sun, H.; Wang, A.; Huang, J.; Su, B.; Wang, R. National and provincial population projected to 2100 under the shared socioeconomic pathways in China. *Clim. Chang. Res.* **2017**, *13*, 128–137.
46. Jiang, T.; Su, B.; Huang, J.; Zhai, J.; Xia, J.; Wang, Y.; Sun, H.; Luo, Y.; Zhang, L.; Wang, G.; et al. Each 0.5 °C of warming increases annual flood losses in China by more than US \$60 billion. *Bull. Am. Meteorol. Soc.* **2020**, *101*, E1464–E1474. [[CrossRef](#)]
47. Su, B.; Huang, J.; Fischer, T.; Wang, Y.; Kundzewicz, W.; Zhai, J.; Sun, H.; Wang, A.; Zeng, X.; Wang, G.; et al. Drought losses in China might double between the 1.5 °C and 2 °C warming. *Proc. Natl. Acad. Sci. USA* **2018**, *115*, 10600–10605. [[CrossRef](#)] [[PubMed](#)]
48. Wang, Y.; Wang, A.; Zhai, J.; Tao, T.; Jiang, T.; Su, B.; Yang, J.; Wang, G.; Liu, Q.; Gao, C.; et al. Tens of thousands additional deaths annually in cities of China between 1.5°C and 2.0 °C warming. *Nat. Commun.* **2019**, *10*, 3376. [[CrossRef](#)] [[PubMed](#)]
49. Xu, Z.X. *Hydrological Models*; Science Press: Beijing, China, 2009.
50. Krysanova, V.; Bronstert, A.; Müller-Wohlferl, D.I. Modelling river discharge for large drainage basins: From lumped to distributed approach. *Hydrol. Sci. J.* **1999**, *44*, 313–331. [[CrossRef](#)]

51. Zhao, H.; Zhang, Y.; Wang, Z.; Mao, Y.; An, W. Threshold of precipitation for Qinhe River Flood based on HBV model. *Res. Soil Water Conserv.* **2015**, *22*, 74–78. (In Chinese)
52. Zhang, T.; Zhao, Q.; Shi, X.; Ma, Z. Application of HBV model on estimating critical rainfall of flood disaster in Longwu River. *J. China Agric. Univ.* **2017**, *22*, 69–75. (In Chinese)
53. Wang, X.; Yang, T.; Wang, B.; Li, H.; Hao, X. Scenarios forecasting of runoff extreme values in source region of Yellow River Basin on multiple hydrological models. *Water Resour. Power* **2012**, *30*, 27–30. (In Chinese)
54. Liu, L.; Xu, H.; Wang, Y.; Jiang, T. Impacts of 1.5 and 2 °C global warming on water availability and extreme hydrological events in Yiluo and Beijiing River catchments in China. *Clim. Chang.* **2017**, *145*, 145–158. [[CrossRef](#)]
55. Liu, L.; Xiao, C.; Du, L.; Zhang, P.; Wang, G. Extended-Range Runoff Forecasting Using a One-Way Coupled Climate–Hydrological Model: Case Studies of the Yiluo and Beijiing Rivers in China. *Water* **2019**, *11*, 1150. [[CrossRef](#)]
56. Doherty, J.; Johnston, J. Methodologies for calibration and predictive analysis of a watershed model. *J. Am. Water Resour. Assoc.* **2003**, *9*, 251–265. [[CrossRef](#)]
57. Bahremand, A.; Smedt, F. Distributed Hydrological Modeling and Sensitivity Analysis in Torysa Watershed, Slovakia. *Water Resour. Manag.* **2008**, *22*, 393–408. [[CrossRef](#)]
58. Falkenmark, M.; Lundquist, J.; Widstrand, C. Macro-scale Water Scarcity Requires Micro-scale Approaches: Aspects of Vulnerability in Semi-arid Development. *Nat. Resour. Forum* **1989**, *13*, 258–267. [[CrossRef](#)]
59. Schewe, J.; Heinke, J.; Gerten, D.; Haddeland, I.; Arnell, N.; Clark, D.; Dankers, R.; Eisner, S.; Fekete, B.; Colón-González, F.; et al. Multimodel assessment of water scarcity under climate change. *Proc. Natl. Acad. Sci. USA* **2014**, *111*, 3245–3250. [[CrossRef](#)] [[PubMed](#)]
60. Falkenmark, M. Water scarcity and population growth: A spiralling risk. *Ecodeision* **1992**, *21*, 498–502.
61. Wu, J.; Chen, X.; Yao, H.; Gao, L.; Chen, Y.; Liu, M. Non-linear relationship of hydrological drought responding to meteorological drought and impact of a large reservoir. *J. Hydrol.* **2017**, *551*, 405–507. [[CrossRef](#)]
62. Garcia, P.; Nicolas, A.; Velazquez, M. Combined use of relative drought indices to analyze climate change impact on meteorological and hydrological droughts in a Mediterranean basin. *J. Hydrol.* **2017**, *554*, 292–305. [[CrossRef](#)]
63. Oloruntade, A.; Mohammad, T.; Ghazali, A.; Wayayok, A. Analysis of meteorological and hydrological droughts in the Niger-South Basin, Nigeria. *Glob. Planet. Chang.* **2017**, *155*, 225–233. [[CrossRef](#)]
64. Svoboda, M.D.; Fuchs, B.A. *Handbook of Drought Indicators and Indices* (M. Svoboda and B.A. Fuchs); Integrated Drought Management Programme (IDMP), Integrated Drought Management Tools and Guidelines Series 2; World Meteorological Organization: Geneva, Switzerland, 2016.
65. Mercadeo, V.; Perez, G.; Solomatine, D.; Lanen, H. Spatio-temporal analysis of hydrological drought at catchment scale using a spatially-distributed hydrological model. *Procedia Eng.* **2016**, *154*, 738–744. [[CrossRef](#)]
66. Davison, A.C. Modeling excesses over high thresholds, with an application. In *Statistical Extremes and Applications*; Tiago de Oliveira, J., Ed.; Riedel: Dordrecht, The Netherlands, 1984; pp. 461–482.
67. Kay, A.; Davies, H.; Bell, V.; Jones, R. Comparison of uncertainty sources for climate change impacts: Flood frequency in England. *Clim. Chang.* **2009**, *92*, 41–63. [[CrossRef](#)]
68. Moriasi, D.; Arnold, G.; Kuyik, M.; Bingner, R.; Harmel, R.; Veith, T. Model evaluation guidelines for systematic quantification of accuracy in watershed simulations. *Trans. ASABE* **2007**, *50*, 885–900.
69. Gosling, S.; Taylor, R.; Arnell, N.; Todd, M. A comparative analysis of projected impacts of climate change on river runoff from global and catchment-scale hydrological models. *Hydrol. Earth Syst. Sci.* **2011**, *15*, 279–294. [[CrossRef](#)]
70. Liu, L.; Fischer, T.; Jiang, T.; Luo, Y. Comparison of uncertainties in projected flood frequency of the Zhujiang River, South China. *Quat. Int.* **2013**, *304*, 51–61. [[CrossRef](#)]
71. Vetter, T.; Reinhardt, J.; Flörke, M.; Griensven, A.; Hattermann, F.; Huang, S.; Koch, H.; Pechlivanidis, I.; Plötner, S.; Seidou, O.; et al. Evaluation of sources of uncertainty in projected hydrological changes under climate change in 21 large-scale river basins. *Clim. Chang.* **2015**, *141*, 419–433. [[CrossRef](#)]
72. Vetter, T.; Huang, S.; Aick, V.; Yang, T.; Wang, X.; Krysanova, V.; Hattermann, F. Multi-model climate impact assessment and intercomparison for three large scale river basins on three continents. *Earth Syst. Dyn.* **2015**, *6*, 17–43. [[CrossRef](#)]
73. Hattermann, F.F.; Vetter, T.; Breuer, L.; Su, B.; Daggupati, P.; Donnelly, C.; Fekete, B.; Flörker, F.; Gosling, S.; Hoffmann, P.; et al. Sources of uncertainty in hydrological climate impact assessment: A cross-scale study. *Environ. Res. Lett.* **2018**, *13*, 015006. [[CrossRef](#)]
74. Joseph, J.; Ghosh, S.; Pathak, A.; Sahai, A. Hydrologic impacts of climate change: Comparisons between hydrological parameter uncertainty and climate model uncertainty. *J. Hydrol.* **2018**, *566*, 1–22. [[CrossRef](#)]
75. Wang, Y.; Xu, H.; Li, Y.; Liu, Y.; Hu, Z.; Xiao, C.; Yang, T. Climate Change Impacts on Runoff in the Fujiang River Basin Based on CMIP6 and SWAT Model. *Water* **2022**, *14*, 3614. [[CrossRef](#)]
76. Smith, C.; Nicholls, Z.R.J.; Armour, K.; Collins, W.; Forster, P.; Meinshausen, M.; Palmer, M.D.; Watanabe, M. The Earth’s Energy Budget, Climate Feedbacks, and Climate Sensitivity Supplementary Material. In *Climate Change 2021: The Physical Science Basis; Contribution of Working Group I to the Sixth Assessment Report of the Intergovernmental Panel on Climate Change*; Masson-Delmotte, V., Zhai, P., Pirani, A., Connors, S.L., Péan, C., Berger, S., Caud, N., Chen, Y., Goldfarb, L., Gomis, M.I., Eds.; Cambridge University Press: Cambridge, UK; New York, NY, USA, 2021; Available online: <https://www.ipcc.ch/> (accessed on 20 September 2022).

77. Xin, X.; Wu, T.; Zhang, J.; Yao, J.; Fang, Y. Comparison of CMIP6 and CMIP5 simulations of precipitation in China and the East Asian summer monsoon. *Int. J. Clim.* **2020**, *40*, 6423–6440. [[CrossRef](#)]
78. Wei, L.; Xin, X.; Li, Q.; Wu, Y.; Tang, H.; Li, Y.; Yang, B. Simulation and projection of climate extremes in China by multiple Coupled Model Intercomparison Project Phase 6 models. *Int. J. Clim.* **2022**, *43*, 219–239. [[CrossRef](#)]

Disclaimer/Publisher’s Note: The statements, opinions and data contained in all publications are solely those of the individual author(s) and contributor(s) and not of MDPI and/or the editor(s). MDPI and/or the editor(s) disclaim responsibility for any injury to people or property resulting from any ideas, methods, instructions or products referred to in the content.